

How Metallic are Small Sodium Clusters?

J. Bowlan, A. Liang, and W. A. de Heer

School of Physics, Georgia Institute of Technology, 837 State St. Atlanta, GA, 30332, USA

(Dated: October 26 2010, revised December 24 2010)

Cryogenic cluster beam experiments have provided crucial insights into the evolution of the metallic state from the atom to the bulk. Surprisingly, one of the most fundamental metallic properties, the ability of a metal to efficiently screen electric fields, is still poorly understood in small clusters. Theory has predicted that many small Na clusters are unable to screen charge inhomogeneities and thus have permanent dipole moments. High precision electric deflection experiments on cryogenically cooled Na_N ($N < 200$) clusters show that the electric dipole moments are at least an order of magnitude smaller than predicted, and are consistent with zero, as expected for a metal. The polarizabilities of Na clusters also show metal sphere behavior, with fine size oscillations caused by the shell structure.

By definition, a classical metal is a material which cannot support an internal electric field. An electric field $\mathbf{E}_{\text{ext}}(r)$ applied to a metal object of arbitrary shape will cause the charge density to rearrange so that $\mathbf{E}_{\text{int}} = 0$. A caveat of this property is that a metallic object cannot have a permanent electric dipole moment (or any other moment), since this implies that there is a non-vanishing internal electric field [1]. This property of metals applies on the macroscopic level, but it is not *a priori* obvious that it applies to extremely small objects such as metal clusters. The effectiveness of the screening can be experimentally tested by measuring the electric dipole moments and polarizabilities.

Early experimental and theoretical work on metal clusters focused on the static dipole polarizability and demonstrated that alkali metal clusters could be approximately treated as small metal spheres [2]. This led to the well-known jellium model which allowed a self-consistent description of the electronic shell structure of small clusters. The spherical jellium model predicts that the polarizability of an alkali cluster is $\alpha(N) = (R + \delta(N))^3$, where $R = r_s N^{1/3}$ is the classical cluster radius, r_s is the Wigner-Seitz radius, N is the cluster size (in atoms). $\delta(N)$ is a quantum correction to the radius, often referred to as the spillout factor since it indicates that the electronic screening actually extends beyond the classical cluster radius. To first order, $\delta(N)$ is constant and comparable to the Lang-Kohn value for jellium surfaces [3]. In more sophisticated calculations, $\delta(N)$ varies with cluster size and shows non-trivial shell structure effects [4–6].

The spherical jellium model is clearly flawed: a small metal cluster is not even approximately spherical [2, 7], and the ionic structure has been shown to have significant effects on the thermodynamic properties, [8, 9] and photoelectron spectra [10]. Nevertheless, many physical properties, including the polarizabilities [11–13] are surprisingly well-described. The existing experimental data on Na cluster polarizabilities only sparsely covers the range of cluster sizes, and the experiments were done at temperatures where the clusters are liquid [8, 9]. How-

ever, as we show here, essential features of the jellium model are still observed even in high precision measurements, at cryogenic temperatures where the clusters are expected to be rigid with few or no excited vibrations (20 K).

Electric dipole moments are also expected to be highly sensitive to the electronic screening, and dipole moments have been observed in many metal cluster systems (e.g. Nb, V, Ta [14, 15], and Sn and Pb [16, 17]). An asymmetric cluster without inversion symmetry is expected to have an electric dipole moment, and its magnitude depends on how effectively the charge inhomogeneity of the ion cores is screened by the valence electrons. In the case of Pb clusters, the link between reduced screening and dipole moments is supported by a recent experiment [18] which found reduced core-hole screening in the same size range where dipole moments were observed [17] [19]. For small clusters this reduced screening has been explained as a consequence of partial localization of the electrons due to change in the bonding character and low coordination [18]. An all-electron quantum chemical calculation has predicted that similar effects will lead to dipole moments in Na clusters [20]. Our experiment shows that the electric dipole moments are much smaller, and that metallic screening is not well described by theory even for a cluster as small as Na_3 . The failure of theory to correctly describe static screening in metal clusters is a serious outstanding problem.

Electric dipole moments and polarizabilities are ideally measured using cryogenic molecular beam deflection methods. A beam of neutral metal clusters is produced, deflected and detected using methods that have been previously described [2] (see Refs. [14, 15] for experimental details and parameters). Briefly, cryogenically cooled sodium clusters are produced in a laser vaporization (Nd:YAG 532 nm; 5 mJ/pulse) cluster source operating at 20 K. The beam velocity is measured with a mechanical chopper. The cluster beam is collimated (0.1 mm slits) and passes through the pole faces of an inhomogeneous electric field ($E = 85$ kV/cm, $dE/dz = 218$ kV/cm²). The clusters then deflect due to the force

caused by the electric field gradient on the electric dipole that has an intrinsic component and an induced component. The induced dipole moment causes a uniform deflection of the cluster beam, while the intrinsic dipole moment (primarily) causes a broadening of the beam (see below for details). The cluster beam then enters a position sensitive time of flight mass spectrometer, that simultaneously measures the mass and deflection for all clusters in the beam. This method has been previously used to measure the electric dipole moments of large polar molecules and clusters [21].

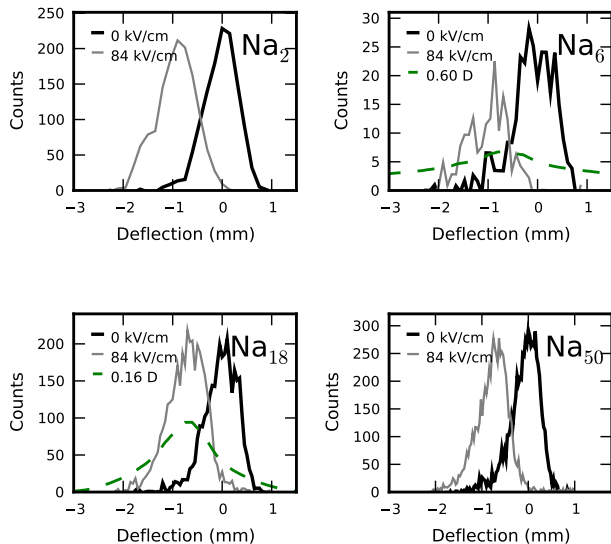


FIG. 1. Electric deflection profiles for Na_N $N=2,6,18$, and 50. The bold line shows the beam profile with the field off, the light line is with the field on. The green dashed curve shows a simulation of the deflection profile using the adiabatic rotor model [22], with the dipole moments calculated in Ref. [20]. For Na_6 a significant depletion of the beam intensity is observed which can be explained by an isomer with a large dipole moment.

For every species in the beam, we measure a distribution of polarizations. We assume that the induced polarization $P = P_\alpha + P_p$ is due to two effects: the electronic polarizability $P_\alpha = \alpha E$, and the dipole moment p projected onto the field, time-averaged over the rotational motion $P_p = \langle p_z \rangle_t$. For a metal spheroid, α is an average of the principal polarizabilities [12]. Because P_p depends on the initial conditions (orientation, energy, and angular momentum) when a cluster adiabatically enters the deflector, the ensemble of clusters shows a distribution of polarizations $\rho(P_p)$. Clusters will in general be deflected toward both the high and low field directions, depending on their initial orientation. The observed deflection profile is thus a convolution of the beam profile with $\rho(P)$, and the signature of the dipole moment is a broadening of the molecular beam, which we measure by $\Delta\sigma = \sqrt{\sigma_{\text{on}}^2 - \sigma_{\text{off}}^2}$. (where $\sigma_{\text{on/off}}$ are the width of the

peaks with the field on or off, respectively)

To derive a quantitative relation between the dipole moment p and the beam broadening $\Delta\sigma$, we use the adiabatic rotor model developed by Bertsch and others [21, 22]. This model uses classical rigid-body mechanics to calculate $P_p = \langle p_z \rangle_t$. For Na_{10} at 20 K, the rotational constant $B = \hbar^2/2I \approx 1\mu\text{eV}$, so $2B/kT \approx 0.001$, thus the rotational levels are effectively continuous, and classical mechanics applies. For a spherical rotor in the $pE/kT \ll 1$ limit, the model predicts a polarization distribution with the analytic form: $\rho(P) = (1/2p) \log |p/P|$ [22]. The variance of this distribution is $p^2/9$ so the deflection profile of a cluster with p will show $\Delta\sigma = p/3$. For our experiment, $p = 0.1$ D, gives $pE/kT \approx 0.01$, so the asymptotic regime $pE/kT \ll 1$ applies. The structure of the cluster also affects the deflection profile. For symmetric tops ($R_1 \neq R_2 = R_3$), the quantitative relation between p and $\Delta\sigma$ is slightly different when $pE/kT \ll 1$. Simulations for $R_1/R_3 = 1.4$ show that the relation $p = 3\Delta\sigma$ holds to within 7%. Na clusters are known to show triaxial distortions, and there has been experimental and theoretical work [23] suggesting that a polar asymmetric rotors will tumble chaotically in the field if perturbed. This explanation was invoked to explain deflection experiments on biomolecules [23] with dipole moments of 6 D, that showed reduced broadening. In our laboratory, we have performed deflection experiments on weakly polar, highly asymmetric metal clusters (e.g. the planar Au_9 cluster (0.28 D) [24]) and observed no evidence of chaotic tumbling. In this case, the beam is still symmetrically broadened just as in the symmetric top case, and the $p = 3\Delta\sigma$ estimate agrees with the value from multiple quantum chemical calculations. The model also assumes that any dipole moment is fixed in the clusters structure, and that the cluster is a rigid object. At 20 K, the clusters are well below both the melting temperature and the range of temperatures where softening effects like premelting are known to occur [8, 9].

Per atom p/N and total p dipole moments estimated from the beam broadening using $p = 3\Delta\sigma$ are shown in Fig. 2 Note that p/N scatters around zero for all clusters $N > 20$. For $N < 20$ there is a small amount of residual beam broadening which cannot be explained away as an artifact. [25]. For all of cluster sizes p/N is less than 0.002 D per atom.

The measured dipole moments appear to be greater than 0 for $N < 20$ and Na_3 appears to have the largest p/N . Yet, its total moment is only about 0.01 D. This measured value agrees with the measurements of Ernst [26], and is significantly lower than Ref. [20] which predicts a value of 0.3 D. It should be noted that there is agreement in the overall trend of the measured and calculated dipole moments, which indicates that the calculated shapes could be accurate but that screening is severely underestimated, even for very small clusters. Despite the success of simple shell models, a Na cluster is a many-

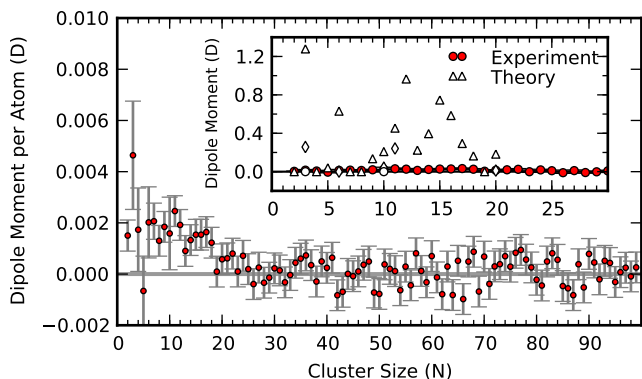


FIG. 2. Experimental dipole moments for Na clusters at 20 K, estimated from the spherical rotor model $p = 3\sqrt{\sigma_{\text{on}}^2 - \sigma_{\text{off}}^2}$. (inset) Comparison between the theoretical dipole moments calculated in Ref. [20] and the experimental values above for small Na clusters. Multiple theoretical values correspond to different isomers, dipole moments of zero (due to symmetry) were predicted for $N=2,3,4,6,7,8,10$, and 19. Thus the discrepancy is greatest for $N = 12-19$. The 1.2 D theoretical value for Na_3 is a high energy isomer that should not be present in our 20 K experiment.

body problem and practical calculations require approximations. Ref. [20] uses a hybrid functional (B3LYP) to treat the exchange and correlation for the calculation of α and p . This method is now known to show serious problems with bulk metallic systems [27]. There are many theoretical methods which deal with the many body problem at lower levels of approximation. Understanding the origin of this error will require a comparison of these methods where the effect of the cluster structure is carefully controlled for. Note that the electrostatic energy of a Na_{20} cluster with a dipole moment of 0.1 D (far larger than what has been measured) is $E = \frac{p^2}{6\epsilon_0 V} \approx 17\mu\text{eV}$. This suggests that correctly calculating the charge density requires high energy accuracy.

Further note that Ref [20] predicts two stable isomers for Na_6 . One is a planar triangle with $p = 0$, while the other is a pentagonal pyramid with $p \approx 0.5$ D. Indeed, the observed intensity loss of Na_6 (Fig. 1) with applied field is consistent with two stable isomers, one which having a much larger p than the other. Experiments are planned to further investigate Na_6 . Note that for all other clusters there is no significant change in the total beam intensity when the electric field is turned on.

We next turn to the high precision polarizability measurements for Na_N $1 \leq N \leq 200$. (Fig. 3). First note that the measurements of $\alpha(N)/N$ generally agree with previous reports. The overall decreasing trend with increasing cluster size agrees with the simple approximation for the polarizability of a conducting sphere with a spillout-enhanced radius $\alpha(N) = (R + \delta)^3$.

Besides the overall decreasing trend, the present measurement also clearly reveals variations in α/N with

the shell structure, which were not previously observed. (Fig. 3) Note that the minima in α/N correspond to spherical shell closings (e.g. $1p^6$ ($N = 8$), $1d^{10}$ ($N = 18$), $1f^{14}$ ($N = 34$), $1g^{18}$ ($N = 58$), $1h^{22}$ ($N = 92$), and within measurement error, $1h^{22}$ ($N = 186$)). However shell closings do not always correspond to minima in α/N . For example, maxima are observed for $2d^{10}$ ($N = 68$), $2f^{14}$ ($N = 106$), and perhaps $2g^{18}$ ($N = 156$). Hence, the systematic trend is, shell closings with principal quantum number 1 are minimum in α/N , and those with principal quantum number 2, tend to be maxima.

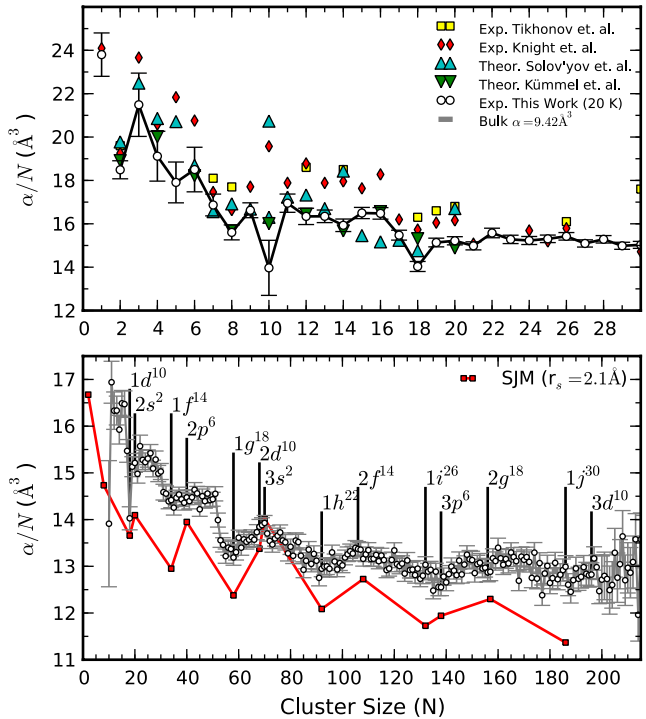


FIG. 3. (upper) α/N of Na_N ($N = 1 - 30$) at a beam temperature of 20 K. Compared with previous higher temperature experiments [11–13] α/N is systematically lower for most sizes and in better agreement with existing theory [20, 28]. $N = 8$ and $N = 18$ are minima as expected for a closed shell. There is also a deep minimum at $N = 10$, (although the variation between experimental runs is larger for $N = 10$). This supports the prolate structure for $N = 10$ as predicted from the Clemenger-Nilsson model [2]. (lower) α/N for Na_N ($N = 10 - 200$) The shell closings have been marked. They coincide with the extrema of the oscillations about the descending trend. At $N = 200$ the clusters are still far from the polarizability of bulk Na metal which is $9.4 \text{ \AA}^3/N$. Shown for comparison is the prediction of the spherical jellium model due to Ekardt [4]

These oscillations in the polarizability with the shell structure were predicted by Ekardt for Na [4], and by Puska and co-workers for Li and Al clusters [5, 6] in the spherical jellium approximation. Puska et. al. [6] qualitatively explain this behavior as follows. By defini-

tion, for an electron in a quantum state with principal quantum number 1, there are no other electrons with the same angular momentum and lower principal quantum number. Consequently, electrons in these shells do not experience the Pauli repulsion from electrons in previously occupied shells with the same angular momentum. Therefore, the orbitals of these electrons penetrate deeper into the cluster and their spillout is reduced. In contrast, electrons in shells with principal quantum number 2 experience the Pauli repulsion from electrons with identical angular momentum in a previously filled shell (for example, electrons in the $2d$ shell are repelled by electrons in the $1d$ shell.) This repulsion enhances the spillout and causes α/N to increase as this shell is filled.

A triaxial distortion can also enhance the axis averaged α of a cluster. However, estimates of the magnitude of this effect using values of the distortion parameter from photoabsorption experiments [7] shows that it is too small to account for the magnitude of the oscillations. It is also noteworthy that, a significant anomaly in the generally smooth trend is observed at $N = 55$. This sudden drop in α/N immediately before the electronic shell closing at $N = 58$, and is likely caused by the geometric shell closing.

Overall the polarizabilities are systematically smaller than reported in previous experiments [11–13], and are in closer agreement with existing theory [20, 28]. This effect has been predicted [29] and is related to thermal expansion. It is surprising that theory gives α to within 5-10%, while the dipole moments are off by orders of magnitude, but this was already nearly the case with the spherical jellium model which has zero dipole moment by symmetry [4].

In conclusion, the electric deflection measurement discussed here gives a comprehensive picture of the response of small sodium clusters to static electric fields. The nearly vanishing electric dipole moments, even for clusters as small as the sodium trimer, demonstrates that the electric fields surrounding alkali clusters are very small, as expected for a classical metallic object. The observed dipole moments are much smaller than predicted by quantum chemical methods, indicating a fundamental challenge for the theoretical treatment of dipole moments in metallic clusters.

We gratefully acknowledge helpful discussions with Xiaoshan Xu. Funding was provided by the NSF under fund No. R7418-DMR-0605894

- [2] W. A. de Heer, *Rev. Mod. Phys.* **65**, 611 (1993).
- [3] N. Lang and W. Kohn, *Phys. Rev. B* **1**, 4555 (1970).
- [4] W. Ekardt *et al.*, *Solid State Communications* **57**, 661 (1986).
- [5] M. Manninen, R. Nieminen, and M. Puska, *Phys. Rev. B* **33**, 4289 (1986).
- [6] M. J. Puska, R. M. Nieminen, and M. Manninen, *Phys. Rev. B* **31**, 3486 (1985).
- [7] M. Schmidt and H. Haberland, *Eur. Phys. J. D* **6**, 109 (1999).
- [8] H. Haberland *et al.*, *Phys. Rev. Lett.* **94**, 35701 (2005).
- [9] C. Hock *et al.*, *Phys. Rev. Lett.* **102**, 43401 (2009).
- [10] O. Kostko *et al.*, *Phys. Rev. Lett.* **98**, 43401 (2007).
- [11] W. D. Knight *et al.*, *Phys. Rev. B* **31**, 2539 (1985).
- [12] G. Tikhonov *et al.*, *Phys. Rev. A* **64**, 63202 (2001).
- [13] D. Rayane *et al.*, *Eur. Phys. J. D* **9**, 243 (1999).
- [14] R. Moro *et al.*, *Science* **300**, 1265 (2003).
- [15] S. Yin *et al.*, *J. Supercond. Nov. Mag.* **21**, 265 (2008).
- [16] S. Schäfer *et al.*, *J. Phys. Chem. A* **112**, 12312 (2008).
- [17] S. Schäfer *et al.*, *J. Chem. Phys.* **129**, 044304 (2008).
- [18] V. Senz *et al.*, *Phys. Rev. Lett.* **102**, 138303 (2009), ISSN 1079-7114.
- [19] Dipole moments were observed in Nb clusters (and 10 alloys) up to $N = 100$. A rigorous theoretical explanation that can account for the loss of screening and all of the related experimental phenomena is currently lacking. See Ref. [15] for more details and references to theoretical work.
- [20] I. A. Solov'yov, A. V. Solov'yov, and W. Greiner, *Phys. Rev. A* **65**, 53203 (2002).
- [21] M. Broyer *et al.*, *C. R. Phys.* **3**, 301 (2002).
- [22] G. Bertsch, N. Onishi, and K. Yabana, *Z. Phys. D Atoms* **34**, 213 (1995).
- [23] M. A. El Rahim *et al.*, *J. Phys. Chem. A* **109**, 8507 (2005).
- [24] J. Bowlan(2010), to be published.
- [25] We have applied corrections for other causes of broadening unrelated to a dipole moment: The dispersion in the beam velocity is negligible. The inhomogeneity of the deflection field causes a small but detectible broadening. This correction accounts for all of the broadening observed in the atomic beams used for calibration (e.g. Li, Al, In).
- [26] L. Coudert, W. Ernst, and O. Golonzka, *J. Chem. Phys.* **117**, 7102 (2002).
- [27] J. Paier, M. Marsman, and G. Kresse, *J. Chem. Phys.* **127**, 024103 (2007).
- [28] S. Kümmel *et al.*, *Eur. Phys. J. D* **11**, 239 (2000).
- [29] S. A. Blundell *et al.*, *Phys. Rev. Lett.* **84**, 4826 (2000).

[1] J. Jackson, *Classical Electrodynamics 3rd ed.* (Wiley, 1998).